

LOW WIND SPEED RADAR BACKSCATTER MEASUREMENTS AT C-  
AND Ku-BAND OBTAINED DURING THE SURFACE WAVES DYNAMICS  
EXPERIMENT

S.C. Carson, J.C. Carswell, R.E. McIntosh  
Microwave Remote Sensing Laboratory  
University of Massachusetts  
Amherst, MA 01003

F.K. Li, S.V. Nghiem, S.H. Lou, and G. Neuman  
Jet Propulsion Laboratory  
California Institute of Technology  
4800 Oak Grove Drive  
Pasadena, CA 91109

David J. McLaughlin  
Northeastern University  
Boston, MA

Submitted to the Journal of  
Geophysical Research

February 1, 1993

## ABSTRACT

Radar backscatter measurements collected at both C- and Ku-Band during the recent Surface Waves Dynamics Experiment (SWADE) on 1 March 1991 show dramatic variabilities of the normalized radar cross section ( $\sigma^0$ ) of the ocean surface at low wind speed. Additionally, measurements of the  $\sigma^0$  in the cross wind direction fluctuated much more than the  $\sigma^0$  in the upwind direction. The C- and Ku- band data are quite similar, both exhibiting a more pronounced roll off of  $\sigma^0$  with decreasing neutral stability wind than indicated by previously published empirical model functions. The data show extremely large azimuthal modulations, in some cases greater than 20 dB, and show good qualitative agreement with the azimuthal modulation predicted by Donelan and Pierson's model function.

## INTRODUCTION

The use of radar scatterometry as a remote sensing technique for measurement of the near surface ocean wind has been demonstrated through a number of airborne and spaceborne experiments [1]. This technique utilizes the relationship between the ocean radar cross section and the near surface wind speed and direction. There are several geophysical models, both theoretical and empirical, in the literature that attempt to describe this relationship. One key area of concern for all of the geophysical models is at low wind speed ( $\leq 4 \text{ ms}^{-1}$ ).

The efficacy of scatterometry at low wind speeds has been debated for a number of years. Donelan and Pierson's model (DP87) predicts a cut-off wind speed dependent upon water temperature, and below which the normalized radar cross section of the ocean surface falls precipitously [2]. Wavetank experiments by Keller et al [3] show an increased variability of the upwind radar cross section at low wind speeds, but do not show a dependence on water temperature. Most geophysical model functions based on empirical studies have been developed with a limited amount of low wind speed cases in the data set. Accurate modelling of the behavior of the radar signature of the ocean surface at low wind speed is assuming greater importance as spaceborne scatterometer monitor the entire earth, including the equatorial region where low wind speed conditions dominate.

Recently the Office of Naval Research (ONR) mounted the Surface Wave Dynamics Experiment (SWADE), which took place off the eastern shore of Virginia between 27 February 1991 and 9 March 1991; NASA sponsored ten flights of a C-Band scatterometer developed at the University of Massachusetts (C-SCAT) and a Ku-Band scatterometer developed at the Jet Propulsion Laboratory (NUSCAT) over the instrumented site of SWADE

on the NASA Ames Research Center's C-130B aircraft. Table 1 summarizes the capabilities of these two radars and figure 1 illustrates their mounting on the C-130B aircraft. Figure 2 shows that the experiment area was instrumented with an array of National Oceanographic and Atmospheric Administration's (NOAA) buoys. These provided meteorological and oceanographic parameters, such as the neutral stability wind speed and the Monin-Obukov stability parameter [4], for comparison with the measurements of normalized radar cross section ( $\sigma^{\circ}$ ) made by the two scatterometers. The Gulf Stream passed through the experiment area causing gradients of sea surface temperature, atmospheric stability and the long wave field. The details of the data analysis will be reported in the future. In this paper, we concentrate on a low wind case study that occurred on 1 March 1991. Figures 3a and 3b show the wind speeds and directions that were measured at buoys A, C and E as a function of time during the data collection period converted to neutral stability at a reference height of ten meters using an algorithm developed by Ezraty [8].

## INSTRUMENTATION

C-SCAT is a pulsed, low-power scatterometer that measures backscatter from the ocean surface at all azimuth angles by rotating a flat microstrip antenna array in a horizontal plane beneath the NASA C-130B aircraft [5]. The main radiation beam of the antenna is pencil-shaped with a beamwidth of approximately 5 degrees. The pointing angle of the main beam can be steered in incidence angle from 20 to 50 degrees off the nadir direction by scanning C-SCAT's transmitting frequency from 5.70 to 4.98 GHz. The transmitted electromagnetic pulses have a peak power of 2 W, and are polarized so that the electric field

	C-SCAT	NUSCAT
Frequency	4.98-5.70 GHz	13.900-13.995 GHz
Polarization	VV	HH HV VH VV
Incidence Angle	20° - 50°	0° - 60°
Azimuth Angle	0° - 360°	0° -360°
Peak Power	2 W	250 W
Antenna Gain	28 dB	32 dB
Beam Width	5°	3°

Table 1 Capabilities of C-SCAT and NUSCAT radars

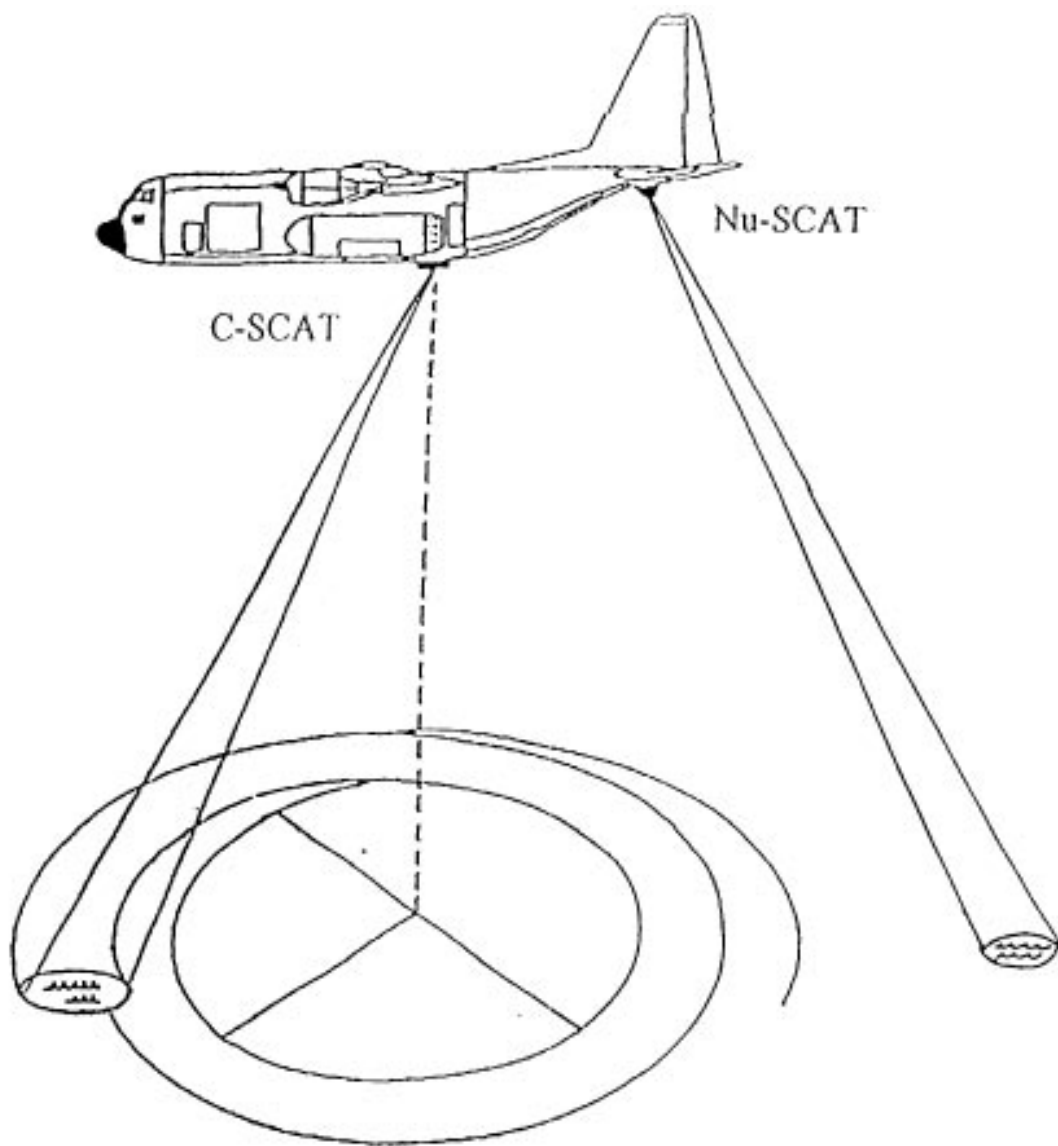


Figure 1 C-SCAT and Nu-SCAT mounted on the NASA-Ames C-130B Aircraft

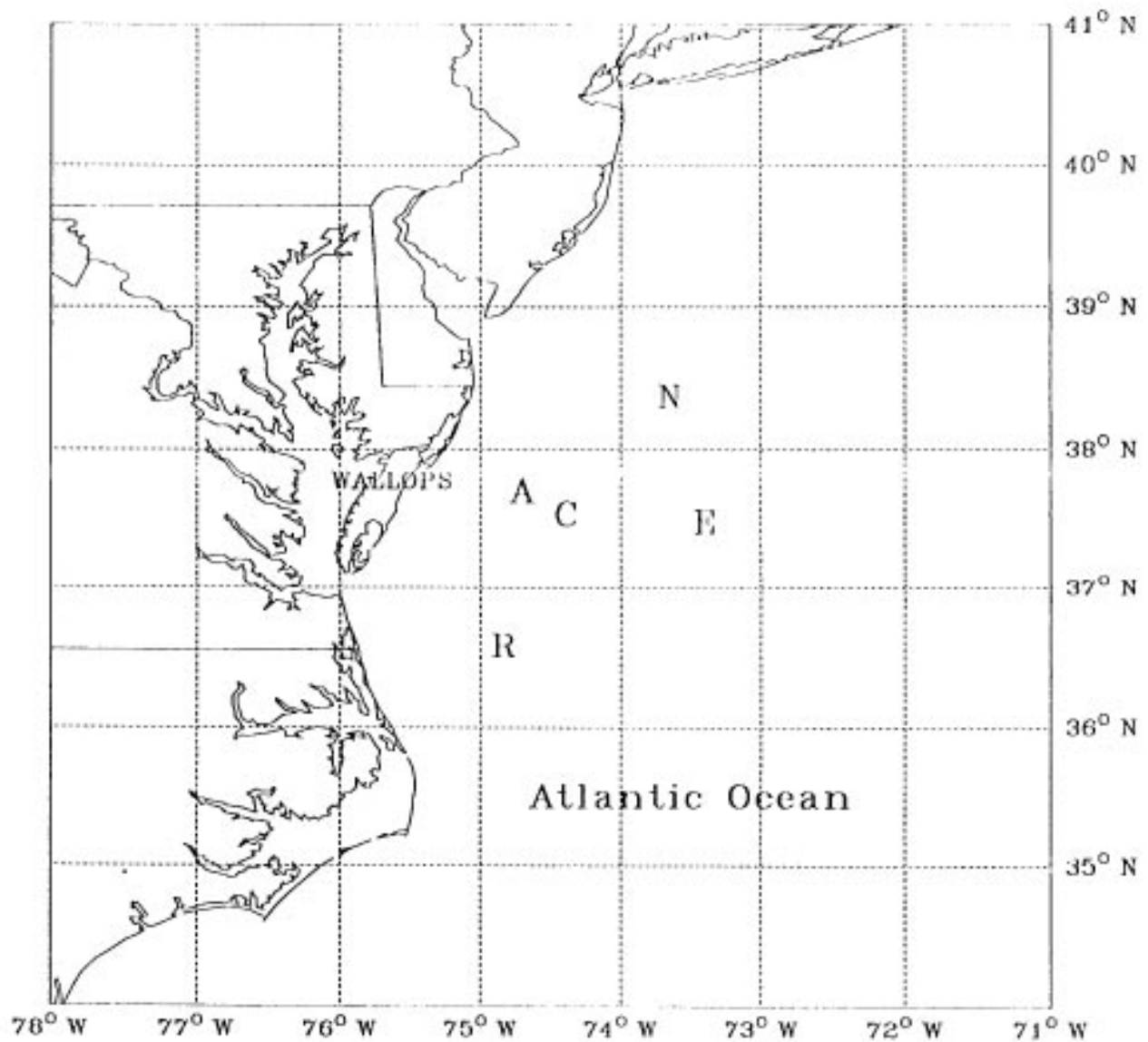
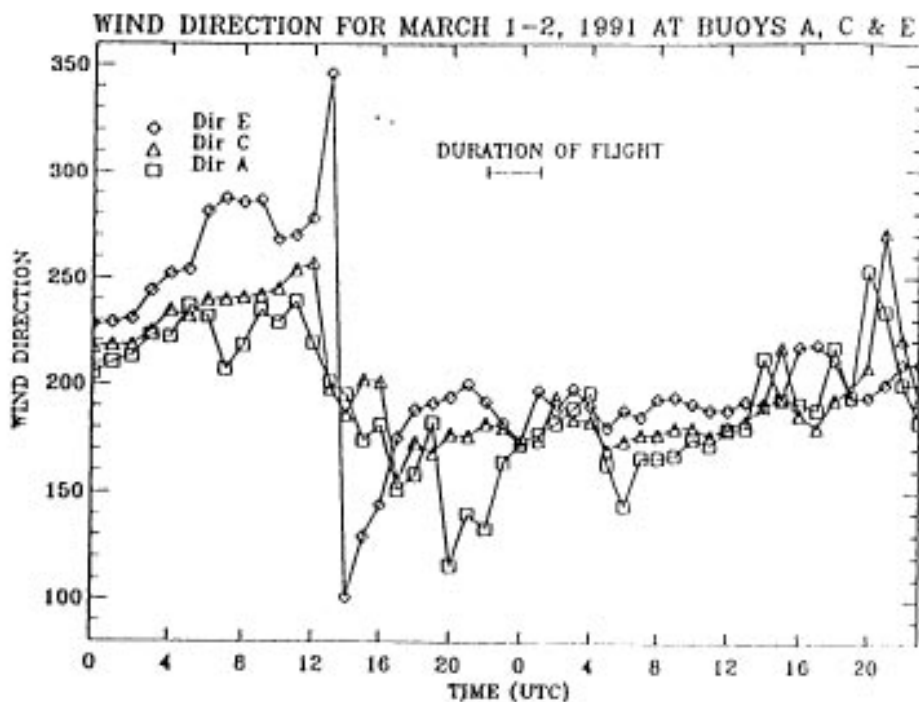
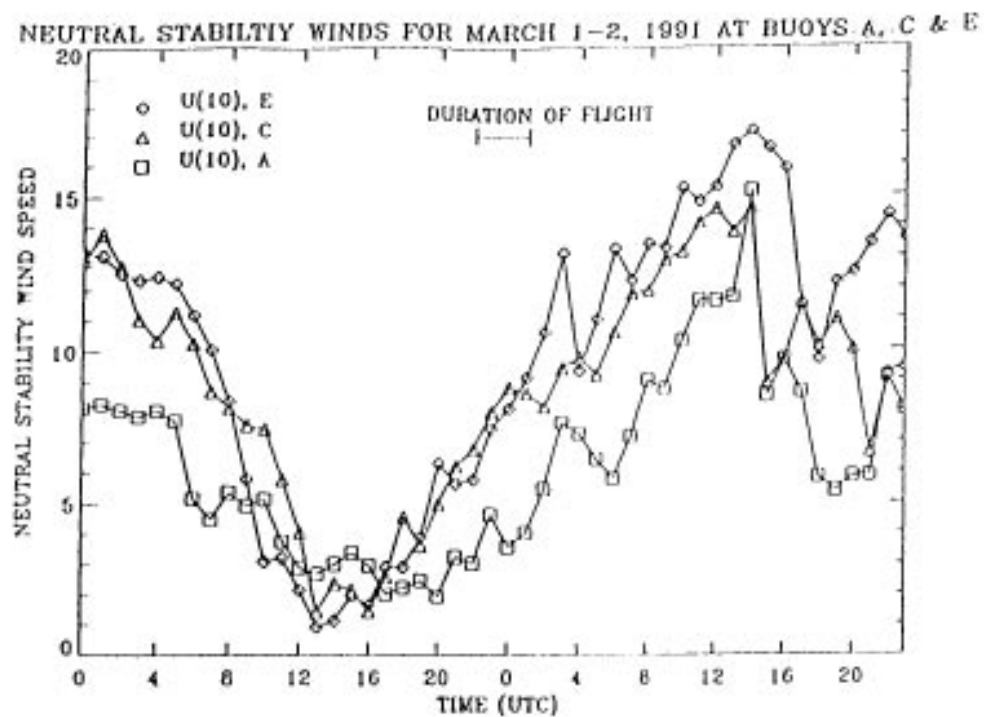


Figure 2 The SWADE experiment area with buoys A (MET 1) , C, E, N and CERC shown. The dashed lines indicate the continental shelf at 200 and 2000 meters.



Figures 3a,b Buoy wind speeds (converted to neutral stability at  $z=10\text{m}$ ) and directions at buoys A, C, and E for March 1-2, 1991

is in the vertical plane. The duration of the transmitted pulses is varied according to the aircraft altitude in order to maximize the signal- to-noise ratio of the backscattered signals.

In order to study the effects of the wind direction on the scatterometer data, the backscattered radar signals were initially averaged into five degree azimuthal data bins. The antenna rotated at 20 rpm, so each rotation collected only 30 independent samples in each five degree bin. The data from at least two azimuthal scans were averaged together to obtain a stable average of the normalized radar cross section.

NUSCAT is also a pulsed scatterometer, transmitting a 14 GHz pulse with peak power of 250 W. This Ku-Band radar uses a gimbal-mounted parabolic dish with a dual polarized feed to measure VV,VH, HV and HH scattering cross sections. While collecting data, the NUSCAT antenna scans by stepping the antenna in ten degree steps in azimuth, taking four seconds of data at each step. The carrier frequency is dithered over 100 MHz to generate additional independent samples. The data are integrated over 1 second intervals. In each 1 second interval, there are ~ 1000 independent samples. This scan technique results in a cycloid scan pattern on the ocean surface from which data is collected.

Both C-SCAT and NUSCAT periodically feed portions of their transmitter output power into the receiver through a series of attenuators to internally calibrate out the system gain fluctuations. C-SCAT is thermally controlled to 300 +/- 1 K in order to minimize gain variations. Typically these are less than 0.1 dB during the course of a flight. Before and after SWADE, C-SCAT was externally calibrated at the University of Massachusetts. The scatterometer was mounted on top of a building, and a 1 m corner reflector was placed in a nearby grassy field. A laser range finder was then used to measure the distance between the corner reflector and the radar. The calibration measurements made before and after SWADE

are within 0.75 dB of each other.

During SWADE, backscatter data was collected with C-SCAT and NUSCAT as a function of the incidence angle of the radar beams on the ocean surface. NUSCAT is capable of measuring backscatter for incidence angles from 0 to 60 degrees, and C-SCAT is capable of measuring backscatter for incidence angles from 20 to 50 degrees. For the flight on 1 March 1992 the antennas of the two scatterometers were coordinated to point in the same incidence angles for all of the measurements described in this paper.

## RESULTS

The experiment on 1 March 1991 consisted of gathering backscatter data at C and Ku-Bands as the aircraft flew twelve passes back and forth between buoys A and C. Figure 3a shows that the wind speed at buoy A was between 3 and 5  $\text{ms}^{-1}$ , and the wind speed at buoy C was  $\sim 8 \text{ ms}^{-1}$ . The backscatter data obtained at both frequencies show that the normalized radar cross section,  $\sigma^0$ , is strongly dependent upon the wind speed during low wind conditions, and the azimuthal modulation of the data due to the wind direction is much greater than data previously reported at this wind speed. Figure 4 shows the normalized radar cross section measured by C-SCAT for a period of 65 seconds during one flight from buoy C to buoy A. Also shown is the azimuthal pointing direction of the C-SCAT antenna, and the number of independent samples obtained for each NRCS value. For this data, the C-SCAT antenna was pointed at 20 degrees off nadir (70 degrees from grazing) and the average signal-to-noise ratio was approximately 24.5 dB. This C-SCAT data shows that the mean  $\sigma^0$  value and its variability as a function of azimuthal angle changes even during this small time

C-SCAT SWADE DATA: MARCH 1

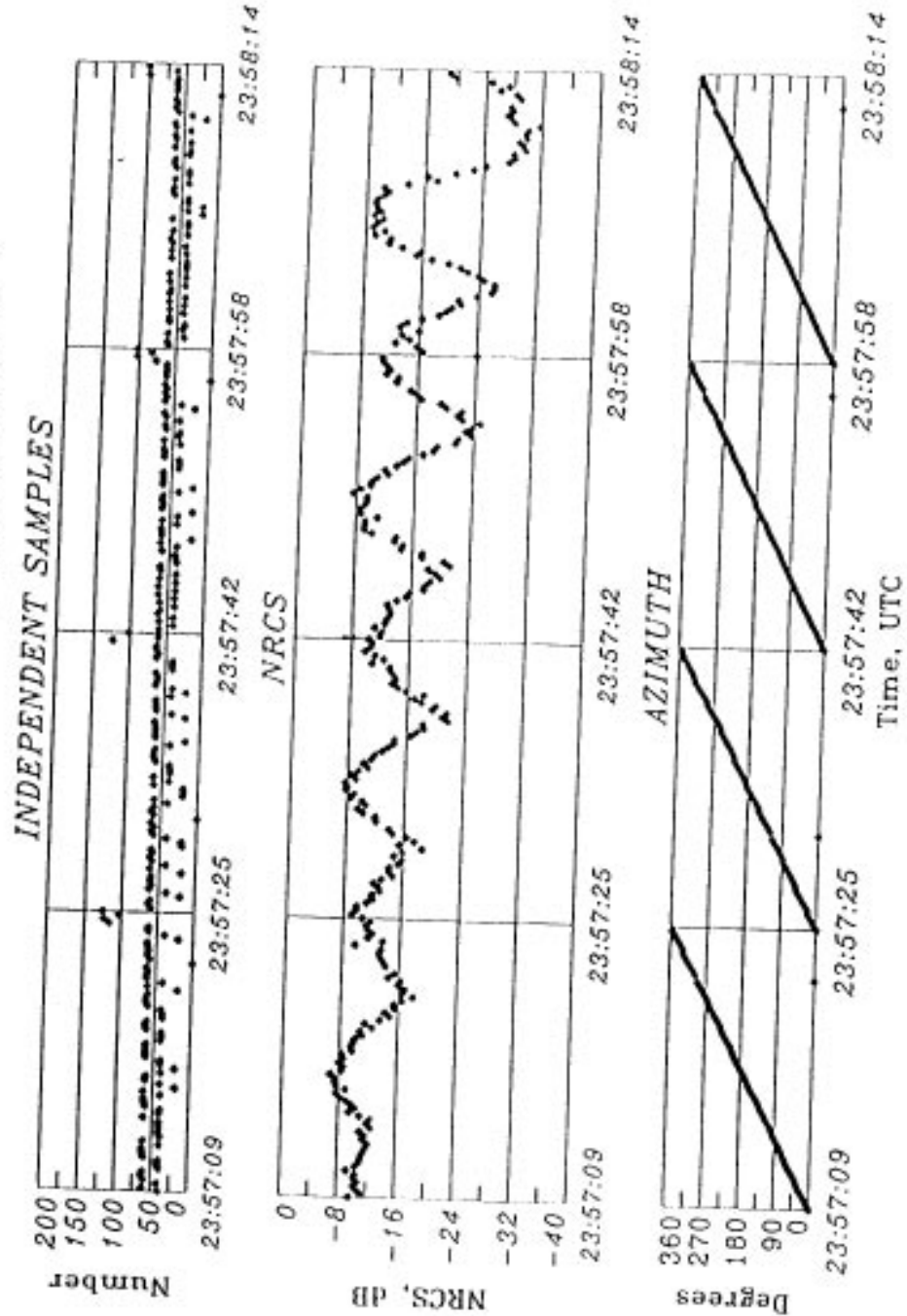
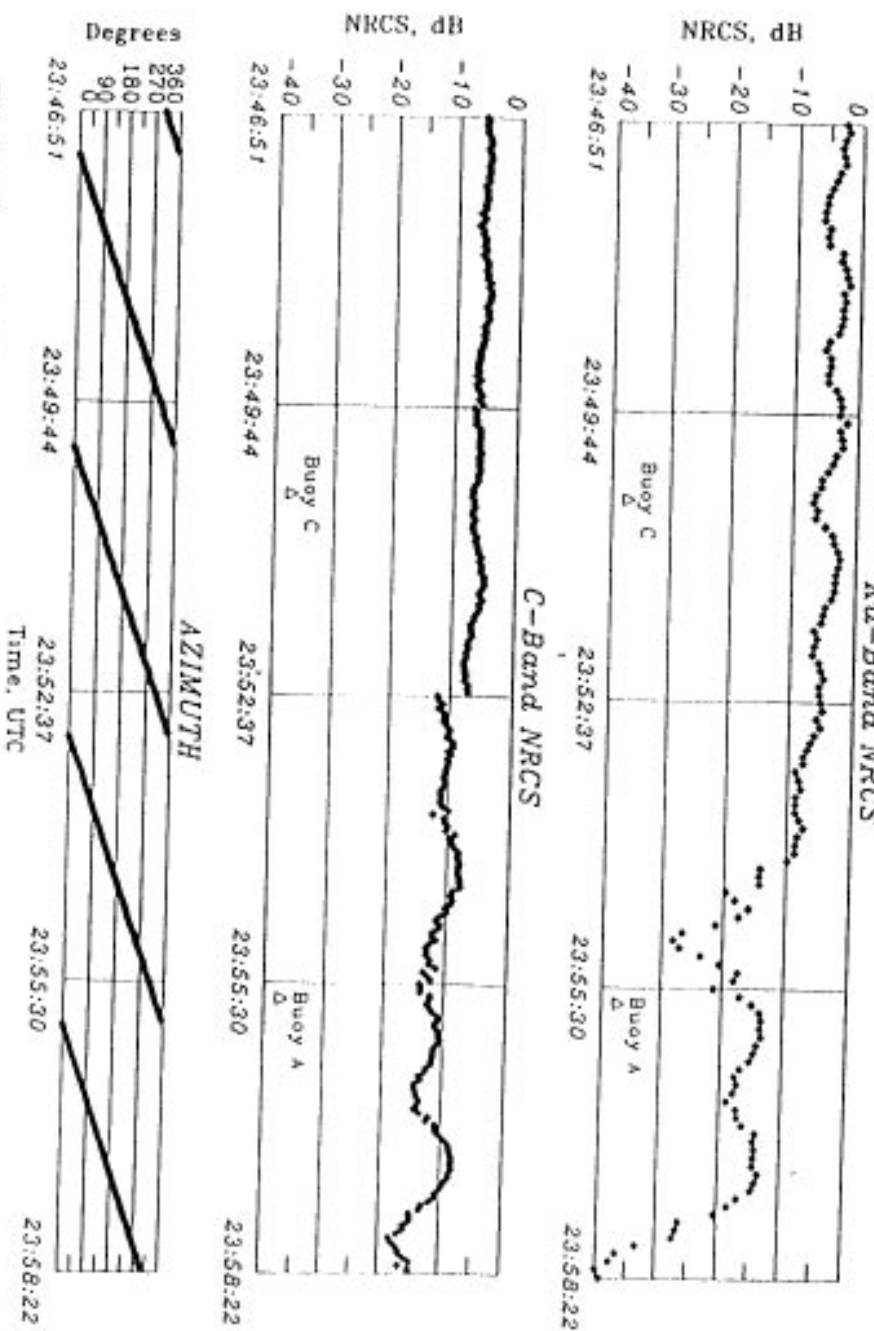


Figure 4 C-SCAT data collected during a 65 second period near buoy  
 A. Note the drop in the cross wind NRCS during this period.

interval, presumably owing to the variability of the wind field and ocean surface conditions over the 7.2 km distance traveled by the aircraft during the 65 seconds of the data time series. Note that the ratio of the peak to the minimum  $\sigma^0$  value varies by more than 20 dB during the last 10 seconds of the data segment. This large variation occurred when C-SCAT was over buoy A, when the neutral stability wind at 10 meters was approximately  $4.0 \text{ ms}^{-1}$ . Strong variations in the Ku-Band  $\sigma^0$  measurements were also observed by NUSCAT during this flights. Figure 5 shows the measured Ku-Band NRCS values during the entire period that it took the aircraft to fly from buoy C to buoy A. The average number of independent samples for each point is  $\sim 1000$  and the average signal to noise ratio is 60 dB. The 25 dB variation of the Ku-Band NRCS during the last 10 seconds of this time series was measured while the C-Band data in figure 4 were collected. The azimuthal scan rate of the C-SCAT antenna was higher than that of the NUSCAT, so in order to compare the data from the 2 radars, the C-Band data was averaged over the time duration of the NUSCAT antenna scan in figure 5. . This averaging reduces the strong azimuthal variations of the C-Band data observed in figure 4, because NRCS data plotted for a specific azimuthal pointing direction of the radar actually contains backscatter samples that correspond to a range of wind speeds and directions because of the wind vector gradient between buoys A and C. This "dispersive" effect increases as NRCS values are obtained by averaging backscatter data over larger areas of the ocean surface. In order to reduce this effect on the NRCS data presented in the remainder of this paper, we average only that amount of backscatter data necessary to achieve statistically stable NRCS measurements. In this manner, we are able to compare the strong azimuthal variations of our measurements to the Donelan and Pierson (DP87), SASS2 and CMOD3-H1 model functions.

*C-SCAT AND Nu-SCAT SWADE DATA: MARCH 1*  
*Ku-Band NRCS*



**Figure 5** C-SCAT and Nu-SCAT data collected during the entire 11 minute, 14 second flight passing over buoys C and A. Note the effects of averaging on the C-Band data.

C and Ku band NRCS measurements were made each time the aircraft passed over buoys A and C during the March 1 experiment. Table 2 summarizes the upwind, downwind, and cross wind  $\sigma^\circ$  values that were measured during eleven different passes at various incidence angles, and Table 3 provides the mean values and the peak to minimum ratios of the  $\sigma^\circ$  for these measurements at each frequency.

To test the validity of the models at low wind speed, the data collected on 1 March 1992 was compared to CMOD3\_H1 [6] at C-Band, SASS-2 [7] at Ku-Band and DP87. CMOD3\_H1 relates the C-Band  $\sigma^\circ$  to the neutral stability wind at 10 m,  $U(10)$ , while SASS-2 uses  $U(19.5)$ , and DP87 uses  $U(\lambda/2)$ , where  $\lambda$  is the Bragg wavelength. An algorithm developed by Ezraty was used to calculate  $U(10)$  from the buoy measurements [8], and then  $U(19.5)$  and  $U(\lambda/2)$  were calculated from  $U(10)$  using (1):

$$U(z) = \frac{U_*}{\kappa} \log \left[ \frac{z}{z_0} \right] \quad (1)$$

The  $\sigma^\circ$  predicted by CMOD3\_H1 and DP87 using the measurements made at buoys A and C and the C-SCAT  $\sigma^\circ$  measurements are shown in figures 6a and 6b for upwind and cross wind, respectively as a function of neutral stability wind speed . Figures 6c and 6d show the  $\sigma^\circ$  predicted by SASS-2 and DP87 for Ku-Band, and the NUSCAT  $\sigma^\circ$  measurements for upwind and cross wind. Only the data within 10 km of the buoys were averaged for this analysis because of the strong spatial gradients between buoys A and C. In order to compensate for the calibration differences between the models and the instruments, the empirical models and the data were normalized to the  $\sigma^\circ$  predicted by DP87 at each frequency for  $20^\circ$  incidence,  $U(10)=8.1 \text{ ms}^{-1}$  and the upwind case. This allows a comparison of the relative changes in  $\sigma^\circ$  in the data with the predicted relative changes predicted by the models.

Table 2A Buoy A: Upwind, downwind and cross wind  $\sigma^{\circ}$  values

Run Number	C-Scat					Nu-Scat				
	Inc. Angle	Up Wind	Cross Wind	Down Wind	Cross Wind	Inc. Angle	Up Wind	Cross Wind	Down Wind	Cross Wind
1	50	-27.6	-46.1	-28.8	-32.3	50	-28.7	-35.6	-31.7	-46.1
2	40	-20.1	-30.5	-23.0	-29.7	40	-26.3	-34.0	-41.8	-39.8
3	30	-11.5	-15.6	-11.4	-17.4	30	-19.6	-30.6	-24.3	-34.6
4	20	-8.9	-26.1	-12.6	-31.7	20	-13.3	-17.1	-13.8	-39.3
5	30	-13.4	-26.7	-13.9	-29.0	10	6.3	-0.2	2.4	0.5
6	40	-20.4	-36.3	-28.9	-37.4	60	N.A.	N.A.	N.A.	N.A.
7	50	-27.3	-34.3	-31.7	-49.2	50	-31.1	-43.5	-25.3	-24.8
8	40	-19.2	-24.0	-22.6	-35.2	40	-25.5	-42.1	-23.8	-32.4
9	30	-13.3	-20.2	-19.5	-13.7	30	-14.7	-15.6	-18.6	-25.1
10	20	-6.8	-14.7	-7.9	-11.6	20	-5.1	-8.3	-7.6	-12.0
11	50	-24.0	-31.5	-26.7	-28.2	50	-28.3	-37.7	-26.1	-29.6

Table 2B Buoy C: Upwind, downwind and cross wind  $\sigma^0$  values

Run Number	C-Scat					Nu-Scat				
	Inc. Angle	Up Wind	Cross Wind	Down Wind	Cross Wind	Inc. Angle	Up Wind	Cross Wind	Down Wind	Cross Wind
1	50	-18.2	-27.8	-20.3	-29.6	50	-15.6	-24.0	-16.4	-19.2
2	40	-13.0	-20.1	-13.9	-20.0	40	-13.8	-20.4	-15.1	-20/2
3	30	-5.3	-11.5	-6.5	-11.2	30	-9.6	-14.0	-10.4	-11.2
4	20	-3.0	-6.8	-4.4	-7.3	20	-1.8	-5.3	-2.8	-5.8
5	30	-6.0	-11.4	-6.9	-9.8	10	7.7	6.3	5.5	4.6
6	40	-13.2	-22.5	-13.9	-21.2	60	N.A.	N.A.	N.A.	N.A.
7	50	-19.2	-26.9	-20.5	-26.5	50	-16.6	-22.4	-17.0	-23.2
8	40	-13.3	-20.2	-19.5	-13.7	40	-14.1	-20.8	-15.5	-20.6
9	30	-3.9	-10.4	-5.7	-10.1	30	-7.9	-13.1	-10.6	-14.2
10	20	-2.6	-5.2	-2.2	-5.4	20	-1.2	-2.3	-1.4	-4.9
11	50	-16.6	-26.0	-19.6	-25.4	50	-14.9	-20.1	-15.7	-18.4

Table 3A Buoy A: Mean and Peak-to-Minimum  $\sigma^o$  values

Run Number	C-Scat			Nu-Scat		
	Inc. Angle	Mean	Upwind/ Crosswind	Inc. Angle	Mean	Upwind/ Crosswind
1	50	-30.5	18.5	50	-31.9	17.3
2	40	-23.7	10.4	40	-31.7	20.2
3	30	-13.6	5.9	30	-24.2	14.7
4	20	-15.0	22.8	20	-15.5	26.0
5	30	-17.2	15.6	10	4.0	6.5
6	40	-27.0	15.9	60	N.A.	N.A.
7	50	-32.0	19.9	50	-23.8	12.4
8	40	-23.4	16.0	40	-28.7	16.6
9	30	-16.7	22.7	30	-17.8	10.4
10	20	-9.7	7.9	20	-7.7	6.9
11	50	-26.7	7.5	50	-27.7	9.4

Table 3B Buoy C: Mean and Peak-to-Minimum  $\sigma^p$  values

Run Number	C-Scat			Nu-Scat		
	Inc. Angle	Mean	Upwind/ Crosswind	Inc. Angle	Mean	Upwind/ Crosswind
1	50	-22.8	1.4	50	-18.2	8.4
2	40	-16.2	7.1	40	-15.2	7.0
3	30	-8.2	5.9	30	-11.2	4.4
4	20	-5.5	4.3	20	-3.2	4.0
5	30	-8.6	5.4	10	6.7	3.1
6	40	-17.8	6.7	60	N.A.	N.A.
7	50	-22.7	7.7	50	-18.8	6.6
8	40	-16.4	6.9	40	-16.8	6.7
9	30	-7.3	6.5	30	-11.0	6.3
10	20	-3.8	3.0	20	-2.3	3.7
11	50	-20.9	9.4	50	-17.1	5.2

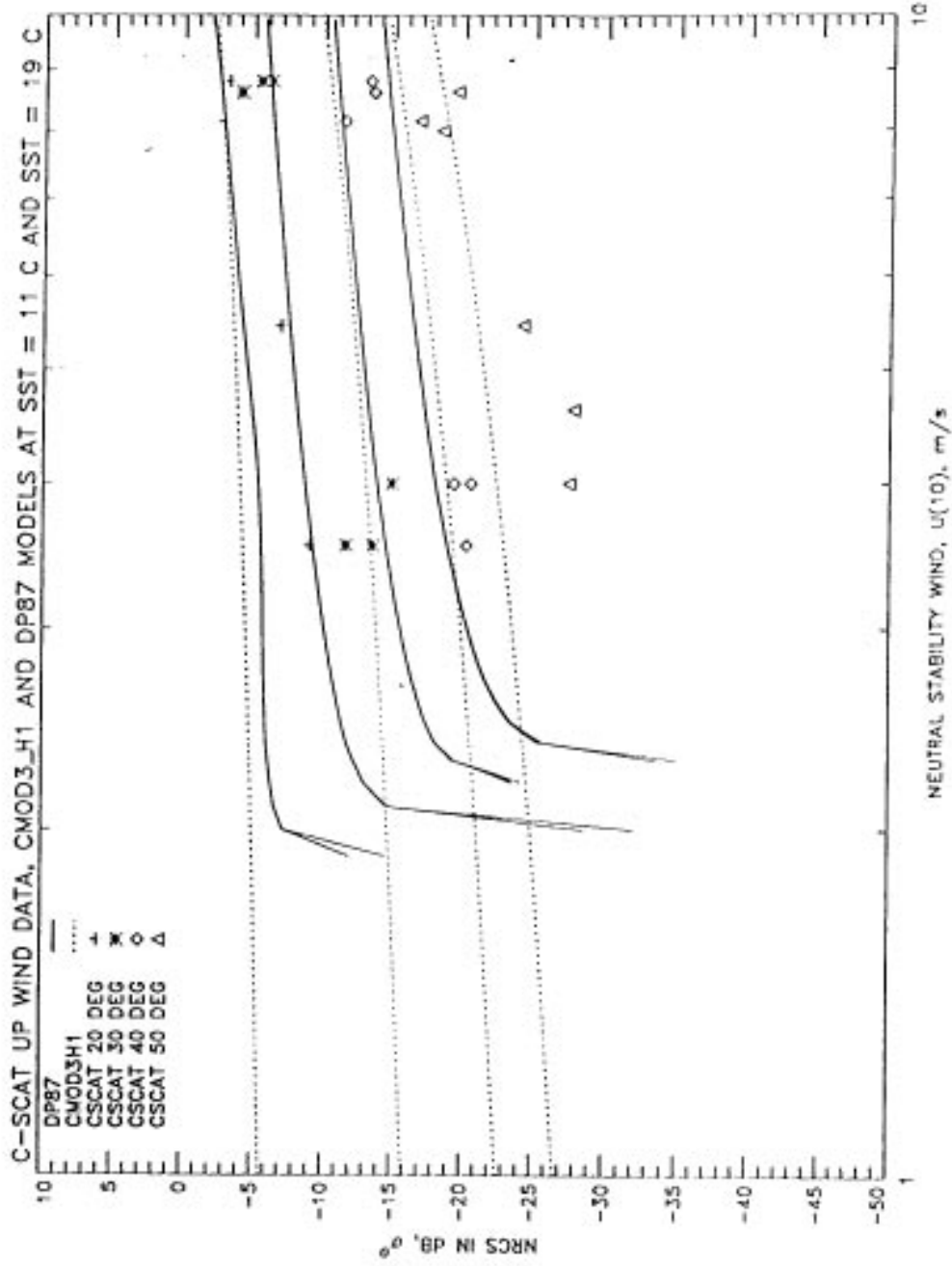


Figure 6a C-SCAT data, CMOD3\_H1 and DP 87 model predictions for up wind at buoy A.

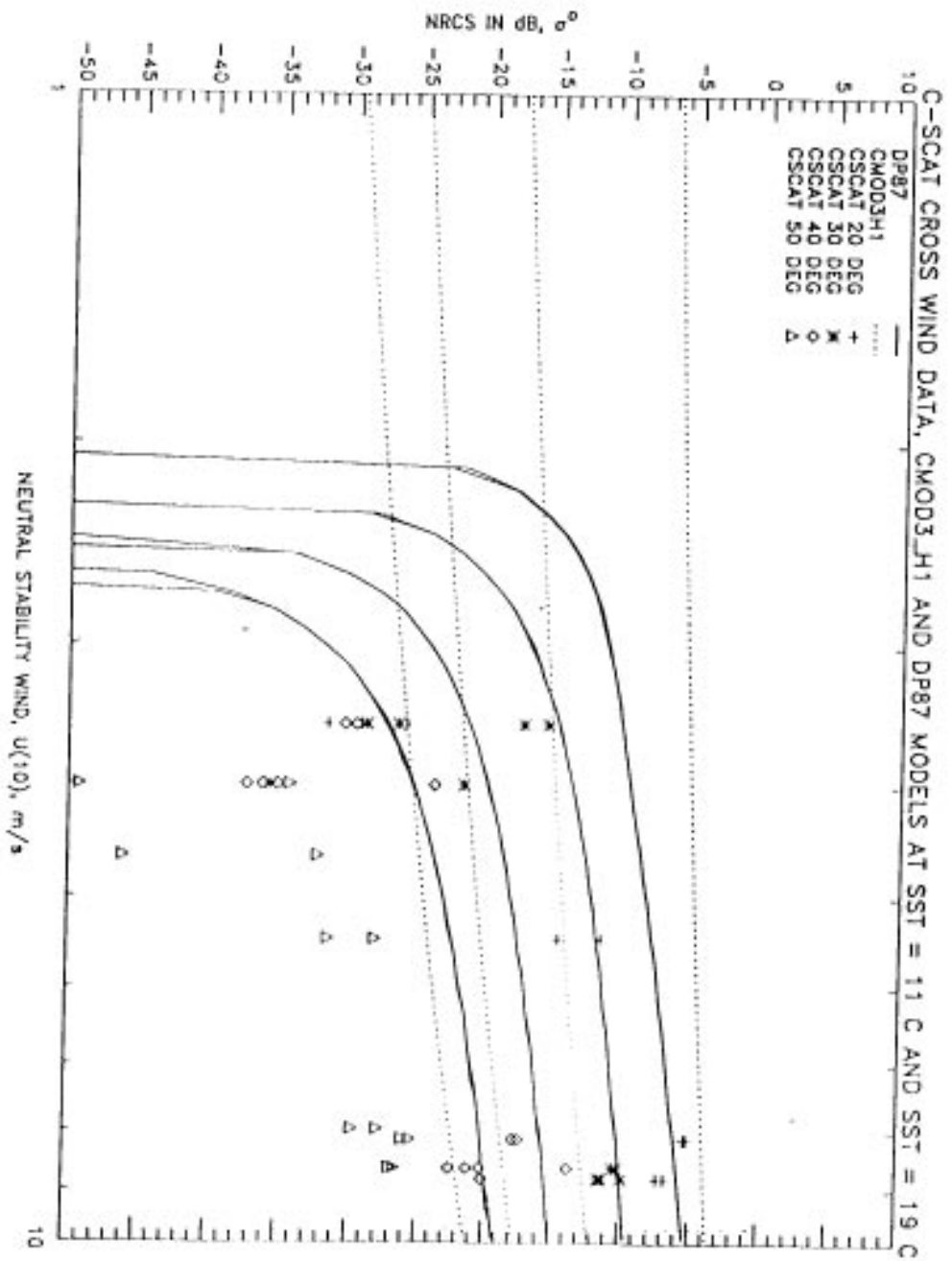
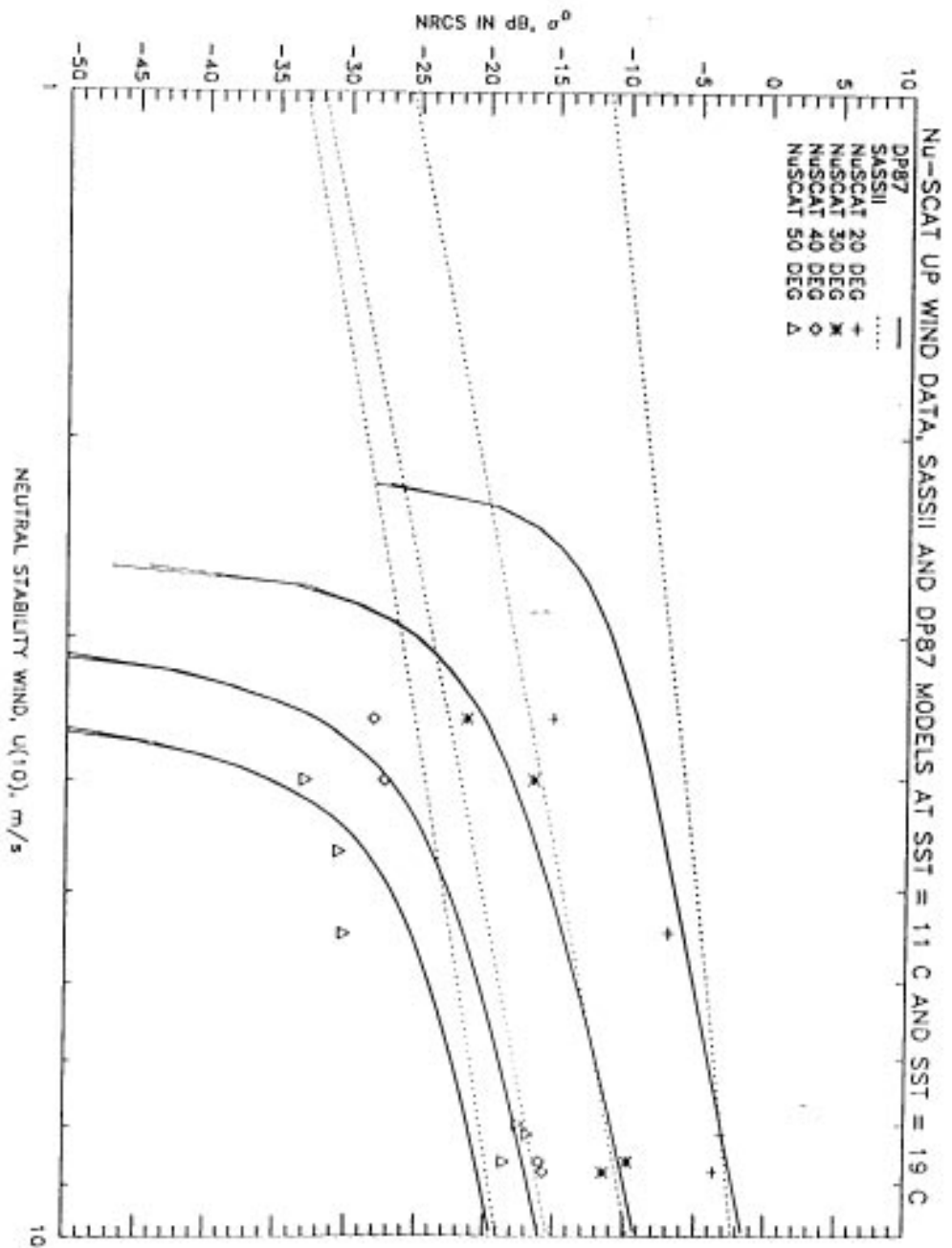


Figure 6b C-SCAT data, CMOD3\_H1 and DP 87 model predictions for cross wind at buoy C.



**Figure 6c** Nu-SCAT data, SASS-2 and DP 87 model predictions for up wind at buoy A.

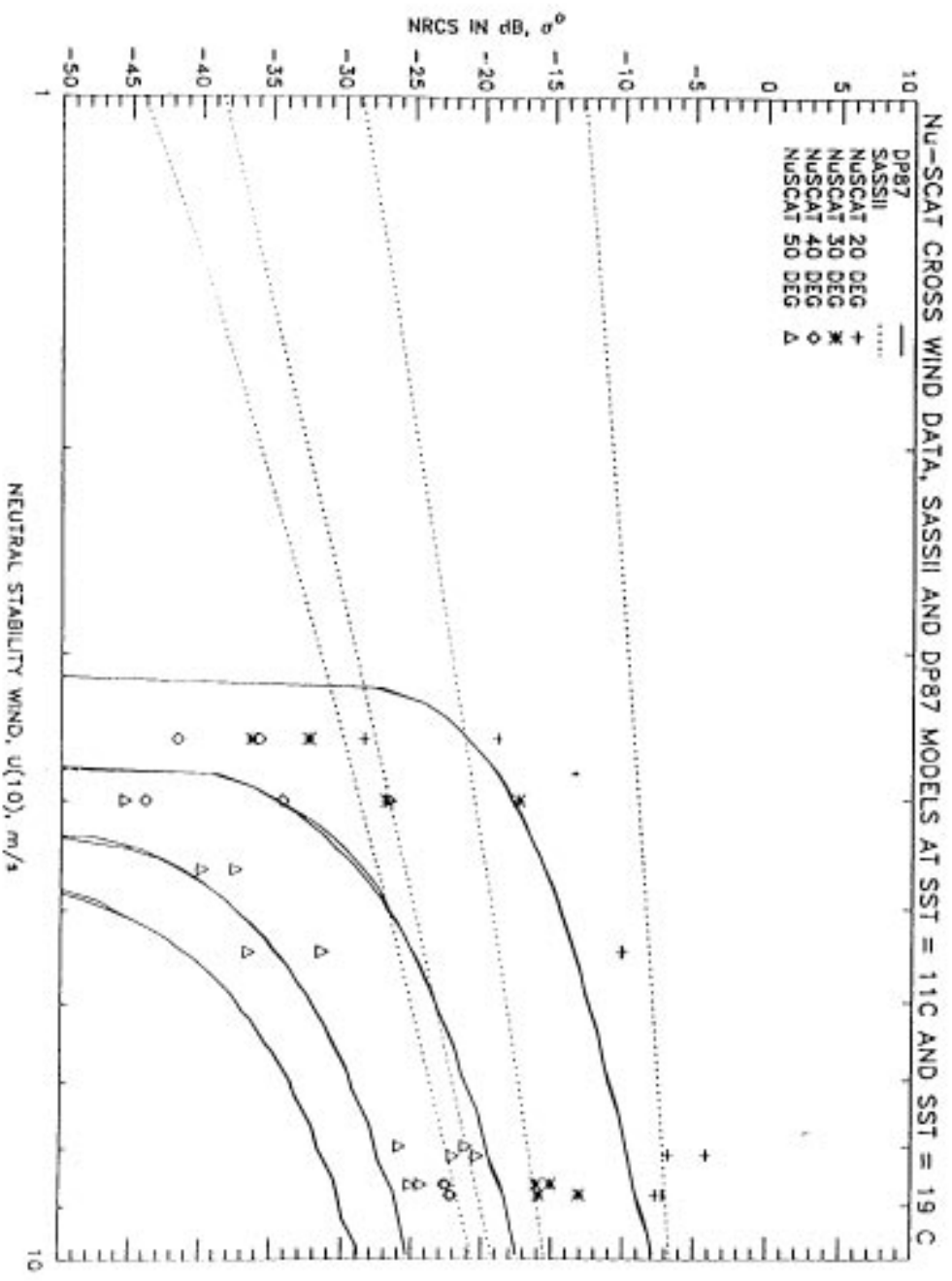


Figure 6d Nu-SCAT data, SASS-2 and DP 87 model predictions for cross wind at buoy C.

Our C and Ku-band measurements made near buoys A do not agree well with the CMOD3-H1 and SASS-2 model functions, respectively. For both our up and cross wind measurements, we observe that the empirical model functions over-estimate the NRCS at low wind speeds. Even though the wind speed measurements made at the buoys may contain significant statistical errors, especially at low wind speeds, those measurement errors can not explain the extremely large and systematic differences between our measurements and the empirical models.

The C-Band data, for both upwind and cross wind, agree with the DP87 model reasonably well at buoy C, where the neutral stability wind speed at 10 m is approximately  $8 \text{ ms}^{-1}$  and the Monin-Obukov stability parameter,  $z/L$ , is nearly zero, but the NRCS values decrease more rapidly with decreasing wind speed than predicted by the models. The greater decrease of the measured  $\sigma^0$  values with wind speed compared to CMOD3\_H1 and DP87 predictions occurs at each incidence angle.

The upwind Ku-Band NRCS data agrees well with the DP87 model at 30 and 40 degrees incidence, but also falls off more with decreasing windspeed at 20 and 50 degrees incidence than predicted by the model. For neutral wind speeds of less than  $5 \text{ ms}^{-1}$ , the Ku-band NRCS drops off drastically with wind speed, especially at cross wind. This is qualitatively consistent with the DP87 model prediction. For cases where  $U(10)$  is greater than  $5 \text{ ms}^{-1}$ , SASS-2 and DP87 show good agreement for the upwind case, but there are considerable discrepancies in the cross wind case.

Figures 7a and b show C-SCAT data over buoys A and C as a function of azimuthal angle and the corresponding predictions of the CMOD3\_H1 and Donelan and Pierson model

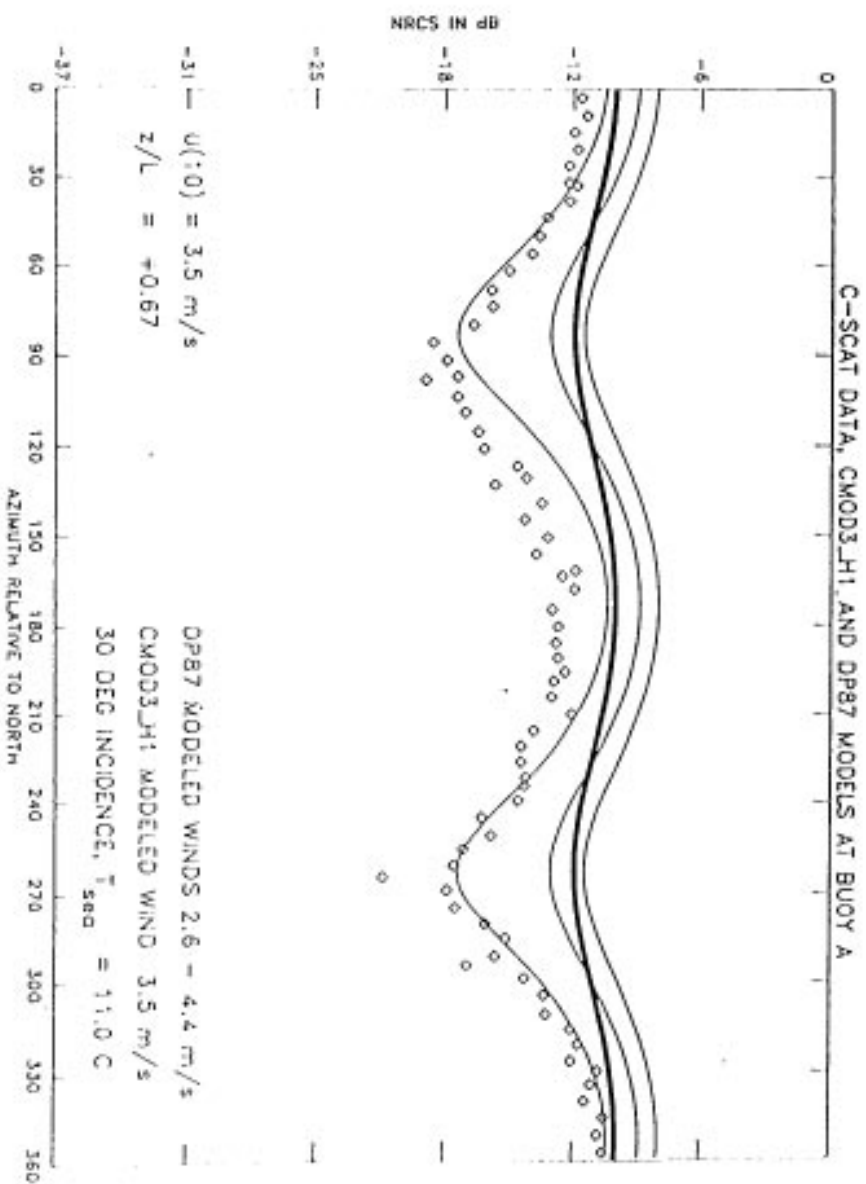


**Figure 7a** C-SCAT data versus azimuth over buoy A. DP87 is shown for a +/- 25 % range of wind speed, and CMOD3\_H1 is the dark line shown  $U(10)=3.5 \text{ ms}^{-1}$ .

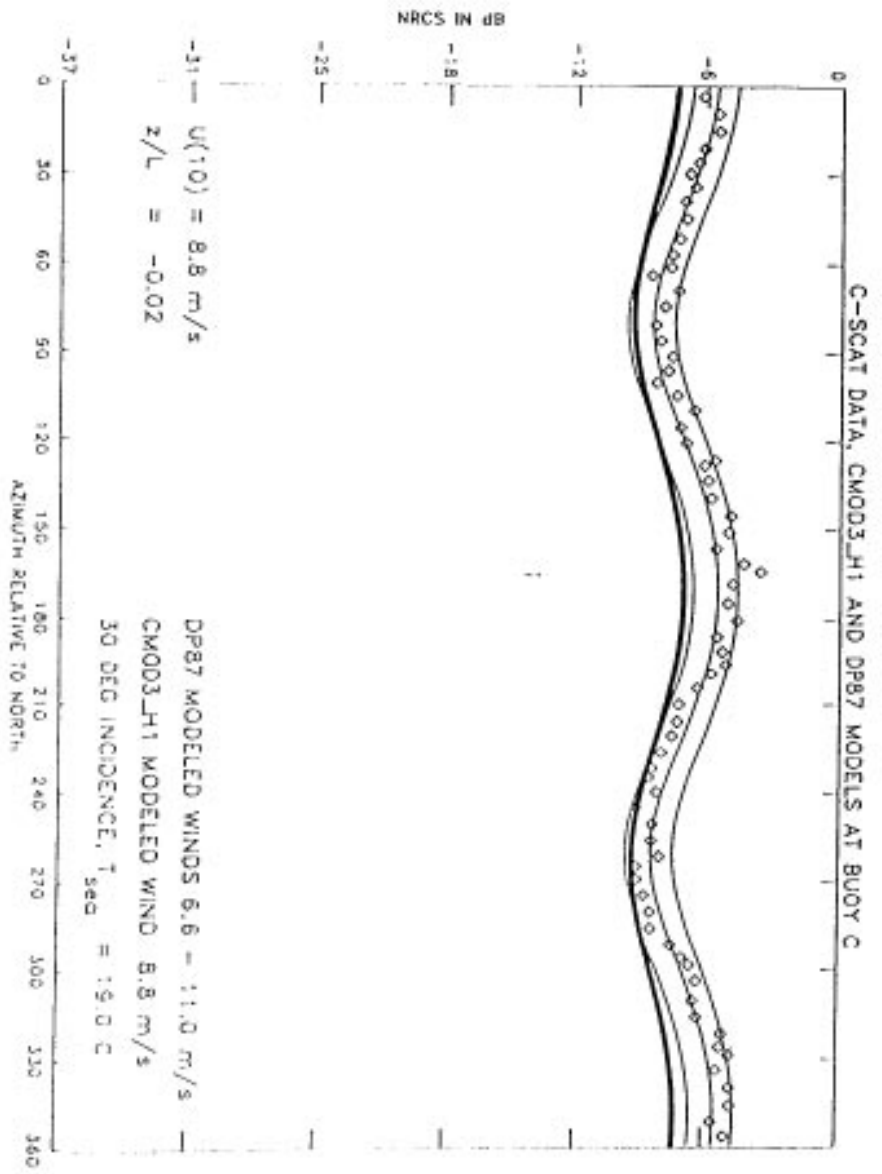


**Figure 7b** C-SCAT data versus azimuth over buoy C. DP87 is shown for a +/- 25 % range of wind speed, and CMOD3\_H1 is the dark line shown  $U(10)=8.8 \text{ ms}^{-1}$ .

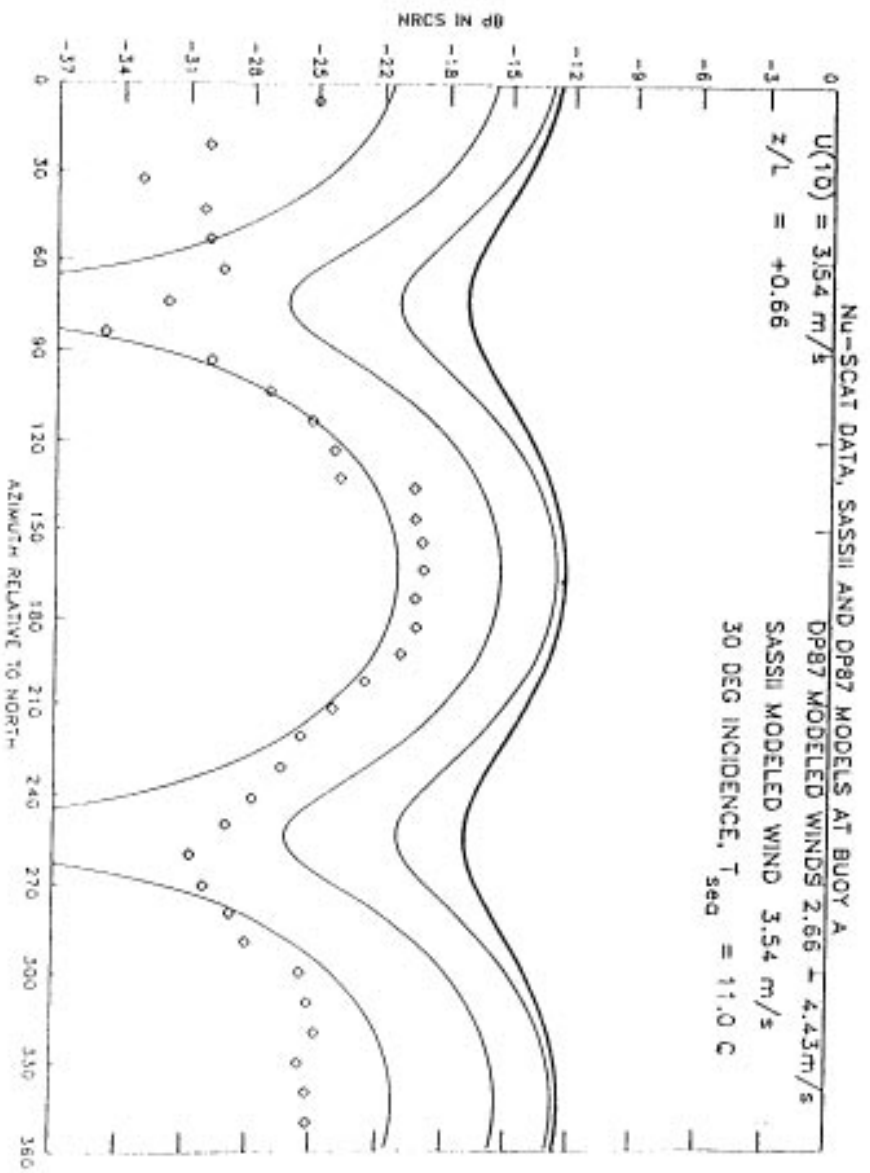


**Figure 7c** Nu-SCAT data versus azimuth over buoy A. DP87 is shown for a +/- 25 % range of wind speed, and SASS-2 is the dark line shown  $U(10)=3.5$   $m s^{-1}$ .

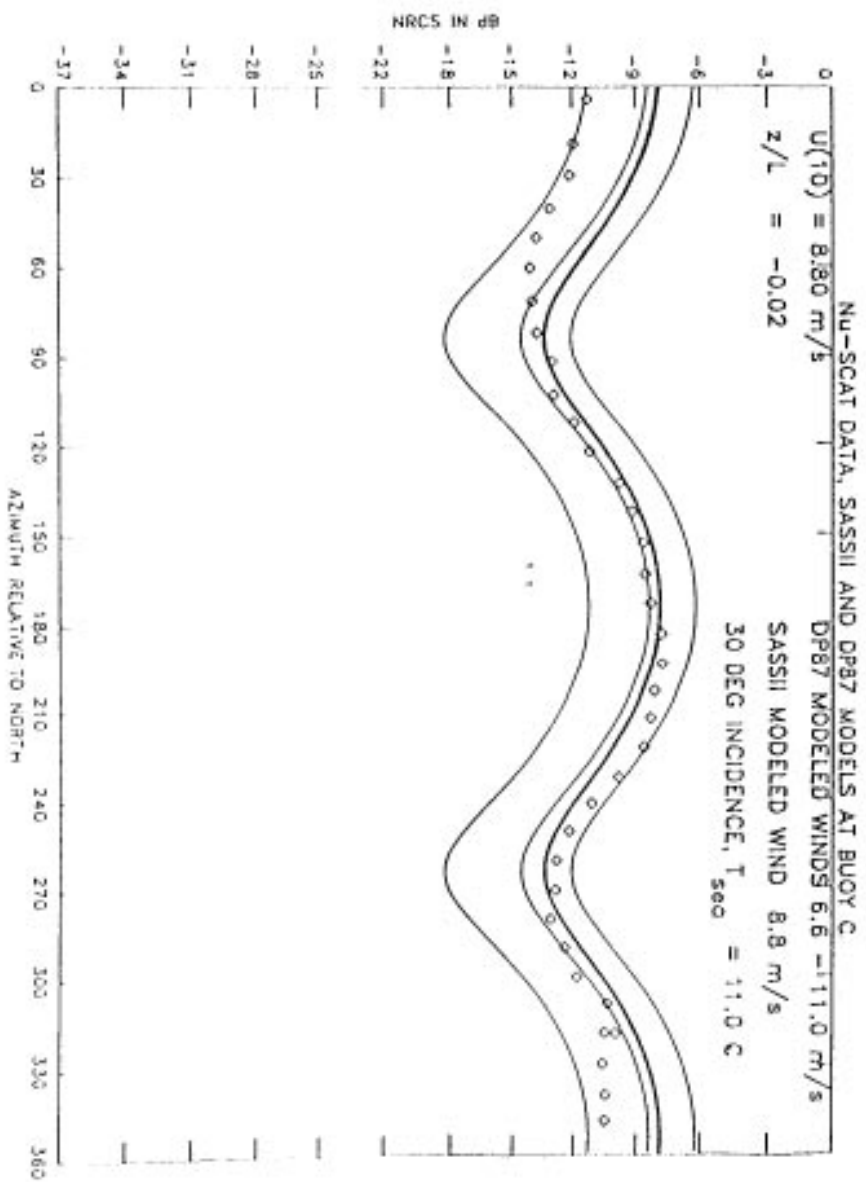


**Figure 7d** Nu-SCAT data versus azimuth over buoy C. DP87 is shown for a +/- 25 % range of wind speed, and SASS-2 is the dark line shown  $U(10)=8.8 \text{ ms}^{-1}$ .

functions. Figures 7c and 7d show Nu-SCAT data and predictions of the SASS-2 and Donelan and Pierson model functions at the same times. The empirical model values were calculated using the neutral winds provided from the buoys. Curves calculated from the Donelan and Pierson model are also shown for these wind speeds as well as for wind speeds 25% above and below the measured values. The NRCS measurements at buoy A were obtained when the winds were  $3.5 \text{ ms}^{-1}$ , which is close to the cutoff wind speed predicted by the DP87 model. We therefore expect that  $\sigma^0$ , particularly in the cross wind direction, is extremely sensitive to errors of the wind estimates. In contrast, the empirical models show only small changes in the amount of azimuthal modulation of the NRCS over the wind speed range from +25 to -25% of the measured wind speed, and they underestimate the azimuthal modulation observed in our data, especially at low wind speeds.

## SUMMARY

The results of the March 1, 1991 SWADE experiment show that the NRCS of the ocean surface falls off dramatically at low wind speeds. NRCS values measured when the radars are pointed in the up-wind and cross-wind directions are generally seen to fall off more with decreasing wind speed than predicted by the empirical CMOD3\_H1 (C-band) or SASS-2 (Ku-band) model functions that were developed primarily from satellite data. The dependence of our measured data on wind speed more closely resembles the Donelan and Pierson model that predicts a threshold windspeed at which the NRCS drops towards zero.

We believe that the resemblance between our measurements and the Donelan Pierson

model compared to the empirical models is due largely to the manner in which the empirical models are developed. C-Band data used to obtain the CMOD3\_H1 model function depended on only three azimuthal looks at the target area for each surface wind measurement, whereas the Ku-band data used to obtain the SASS-2 model function depended on only two azimuthal looks. To generate a model function from such data, it is necessary to average NRCS data for a large number of measurements, for which there are some variations of the wind speeds and directions. These variations are not as important at the higher wind speeds, where the variability of the wind is usually small compared to the mean wind speed. At lower wind speeds, however, the variations do not have to be very large before the azimuthal variations of surface wind model functions are dispersed and the differences between the peak (upwind) and minimum (cross wind) NRCS value are lessened. Additionally, the 50 km resolution of the satellite-based scatterometers causes changes in wind direction on smaller scales to smear the azimuthal pattern of the  $\sigma^0$ , and obscure its decrease with decreasing wind speed. As a result, the CMOD3\_H1 and SASS-2 models agree reasonably well with our data at moderate wind speeds and neutrally stable conditions but they over-predict the average  $\sigma^0$  for stable conditions and low wind speeds, and they under-predict its azimuthal modulation.

The C-band and Ku-band data points presented in this paper were obtained along relatively short flight paths (400m for C-band and 12000m for Ku-band for a full rotation). Consequently, the variability of the wind within the sampled areas were less than if larger sampling areas were used. Nevertheless, some wind variations did occur within the small areas that were simultaneously sampled by the two radars resulting in some averaging effects. These averaging effects will moderate any sharp variations of the NRCS.

If we assume that the variability of the low wind speed measurements are affected by

wind gusts, then fluctuations of the wind speed of the order of 25 % can be applied to the DP model. At  $4 \text{ ms}^{-1}$ , this only amounts to a  $1 \text{ ms}^{-1}$  gust of wind. The DP87 model was tuned using Ku-Band data from RADSCAT, so it is not surprising that it matches the data from NUSCAT better than the data from C-SCAT. However, this model performs better than either of the empirical models for this data set.

The data presented in this paper show a qualitative agreement with the trends of the Donelan and Pierson model function, especially in the predicted drop off of the data in the cross wind direction. Precise quantitative evaluation of the cutoff wind speeds and water temperature effects predicted by the Donelan and Pierson model is not possible with this data set because of the clustering of the environmental parameters, and experimental errors associated with buoy measured winds. Buoys in the open ocean 9 km apart can exhibit an rms discrepancy of 25 % [8], and comparisons of point measurements of wind speed by buoys and radar data are notorious for their scatter. The scatter associated with these measurements limits the quantitative evaluation of DP87.

The data also demonstrate that high resolution scatterometry is essential to validate ocean models, such as the Donelan and Pierson model, as measurements taken over large areas (or averaged over large areas) obscure many features of interest. This, coupled with the relatively small amount of backscatter data collected at low wind speed, may explain why this effect has not been observed in other data sets.

## REFERENCES

- [1] Ulaby, F.T., R. K. Moore, A. K. Fung, *Microwave Remote Sensing, Active and Passive, Volume 2*, Artech House, Norwood, MA, 1986
  
- [2] Donelan, M. A., and W. J. Pierson, "Radar Scattering and Equilibrium Ranges in Wind Generated Waves with Applications to Scatterometry", *J. Geophys. Res.*, Vol. 92, No. C5, May 15, 1987, p 4971.
  
- [3] Keller, M.R., W.C. Keller, and W.J. Plant, "Wave Tank Study of the Dependence of X Band Cross Sections on Wind Speed and Water Temperature", *J. Geophys. Res.*, Vol. 97, No. C4, April 15, 1992, p 5771.
  
- [4] Monin, A.S., A. M. Obukov, "Basic Laws of Turbulent Mixing in the Ground Layer of the Atmosphere", *Tr. Geofiz. Inst. Akad. Nauk. USSR*. Vol. 24, No. 151, p 163, 1954.
  
- [5] McLaughlin, D. J. *Remote Sensing of the Ocean Surface with C-and Ku-Band Airborne Scatterometers*, Ph. D. Dissertation, University of Massachusetts, September, 1989.

- [6] Long, A.E. "C-Band V-Polarized Radar Sea Echo Model from ERS-1 Haltenbanken Campaign", URSI Microwave Signature Conference, IGLS-Innsbruck, Austria, July 1-3, 1992.
  
- [7] Wentz, F.J., S. Peteherych, and L.A. Thomas, "A Model Function for Ocean Radar Cross Section at 14.6 GHz", J. Geophys. Res., Vol. 89, No. C3, 1984, p 3689.
  
- [8] Ezraty, R. "Etude de L'Algorithme D'Estimation de la Vitesse de Frottement a la Surface de la Mer", IFREMER, June 1985, No. 85.2.42.5000, ESA Contract 6155/85/NL/BI.

## TABLES

Table 1	Capabilities of C-SCAT and Nu-SCAT Radars
Table 2A	Buoy A: Upwind, downwind and cross wind $\sigma^o$ values
Table 2B	Buoy C: Upwind, downwind and cross wind $\sigma^o$ values
Table 3A	Buoy A: Mean and Peak-to-Minimum $\sigma^o$ values
Table 3B	Buoy C: Mean and Peak-to-Minimum $\sigma^o$ values

## FIGURES

Figure 1	C-SCAT and Nu-SCAT mounted on the NASA-Ames C-130 Aircraft
Figure 2	The SWADE experiment area with buoys A (MET 1), C, E, N and CERC shown. The dashed lines indicate the continental shelf at 200 and 2000 meters.
Figures 3a,b	Buoy wind speeds (converted to neutral stability at z=10m) and directions at buoys A,C, and E for March 1-2, 1991
Figure 4	C-SCAT data collected during a 65 second period near buoy A. Note the drop in the cross wind NRCS during this period.
Figure 5	C-SCAT and Nu-SCAT data collected during the entire 11 minute, 14 second flight passing over buoys C and A. Note the effects of averaging on the C-Band data.
Figure 6a	C-SCAT data, CMOD3_H1 and DP 87 model predictions for up wind.
Figure 6b	C-SCAT data, CMOD3_H1 and DP 87 model predictions for cross wind.
Figure 6c	Nu-SCAT data, SASS-2 and DP 87 model predictions for up wind.
Figure 6d	Nu-SCAT data, SASS-2 and DP 87 model predictions for cross wind.
Figure 7a	C-SCAT data versus azimuth over buoy A. DP 87 is shown for a +/-25% range of wind speed, and CMOD3_H1 is the dark line shown $U(10)=3.5 \text{ ms}^{-1}$ .
Figure 7b	C-SCAT data versus azimuth over buoy C. DP 87 is shown for a +/-25% range of wind speed, and CMOD3_H1 is the dark line shown $U(10)=8.8 \text{ ms}^{-1}$ .

Figure 7c Nu-SCAT data versus azimuth over buoy A. DP 87 is shown for a  $\pm 25\%$  range of wind speed, and SASS-2 is the dark line shown  $U(10)=3.5 \text{ ms}^{-1}$ .

Figure 7d Nu-SCAT data versus azimuth over buoy C. DP 87 is shown for a  $\pm 25\%$  range of wind speed, and SASS-2 is the dark line shown  $U(10)=8.8 \text{ ms}^{-1}$ .